Treball de Fi de Grau

DOBLE GRAU MATEMÀTIQUES / ENGINYERIA INFORMÀTICA

Facultat de Matemàtiques i Informàtica

Universitat de Barcelona

An EEG Based - Stochastic Dynamical Systems Model of Brain Dynamics

---

David de la Osa Bañales

Directors: Ignasi Cos, Josep Vives

Realitzat a: Departament de Matemàtiques i Informàtica

Barcelona, 13 de juny de 2022

CONTENTS

ABSTRACT

How does the human brain work? How do different brain areas interact with each other when performing specific function? These questions have sharply increased in interest over the last decades, as the more it is known about human cognition and cognitive process distribution the more accurate some procedures will be, such as neuro-pathologies diagnosis, prediction of reaction to stimuli or influence of motivation/rewards on decisions. To analyse human cognition, neuroimaging techniques are commonly used, like Functional Magnetic Resonance Imaging (fMRI), Magnetoencephalography (MEG) or Electroencephalograms (EEGs).

The aim of this project is to build a theoretical model, able to capture the neural dynamics of cortical interactions, which we referred to as effective connectivity. Neural data are high-density EEGs, recorded during a decision-making task (*Cos et al. 2022).* This approach overcomes the limitations that are presented when directly using correlation based connectivity metrics. The framework we created consists of a model-based whole-brain effective connectivity, based on the multivariate Ornstein-Uhlenbeck (MOU) process (MOU-EC). The goal of the model, once fitted, is to provide a directed connectivity estimate that reflects the dynamical state of the EEG signals and a method to generate signals that follow the connectivity.

1 INTRODUCTION, MOTIVATION, OBJECTIVES, COSTS

Electroencephalograms (EEGs) are potent tool to record brain activity. The advantage that EEGs provides over other neuroimaging techniques is that, since they measure relative electrical activity at cortical layers of the brain, they provide a high time resolution (up to 1 sample per millisecond) and therefore they excel at analysing brain reactions when subjects are presented with visual and/or audio stimuli. On top of that, the cost of the machine necessary to record EEGs is considerably cheaper than machines needed to record other neuroimaging techniques like MRI, both in purchase and maintenance, and the training of the professionals to operate them is not as exhausting and complex. Another advantage EEGs provide is that their machine is extremely portable, making them outstanding for doing field work.

Our objective is a model of whole-brain effective connectivity fitted with EEG data. The generative model used is the multivariate Ornstein-Uhlenbeck (MOU). The procedure to obtain the effective connectivity using this model has already been applied to fMRI data in the articles *Gilson et al., 2016*, *Pallarés et al., 2018* and *Gilson et al., 2020*. When the model parameters have been tuned in, the MOU process can simulate the dynamical state of the signals under those regimens. In this project, an auspicious method is expected to be obtained by tweeking the model to handle EEG data.

2 IMPLEMENTATION AND METHODOLOGY

2.1 Data meaning and treatment

The EEG data which is used in this project comes from the article *Cos et al., 2022*. In that article, EEGs were used to record subjects performing under three different motivational states. The test subjects were presented to consisted of two targets, between which they had to choose one and reach to it as fast and precise as possible. In some situations, subjects were required to stop at their target (referred as “stop-in”) while, in others, they were asked to hit their target and cross over it (referred as “cross-over”). The different motivational states were triggered by making the subject perform on their own, side-by-side with a less accurate simulated partner and side-by-side with a more accurate simulated partner. In the article, these motivational states are referred as “solo”, “easy” and “hard”, respectively. It is said as well that partners are there to provide companionship, not competition, so the motivation is generated purely by intrinsic arousal.

60 electrodes were used to record each of the regions of interest (ROIs) on the cortical surface, distributed following a generic pattern to estimate the location of these electrodes for a 60-electrode Acticap configuration and, after eliminating noisy and artefactual sources, the source spaces had a dimension from 40 to 50 sources, varying from subject to subject (*Fig. 1: Stage 1, Fig. 2*).

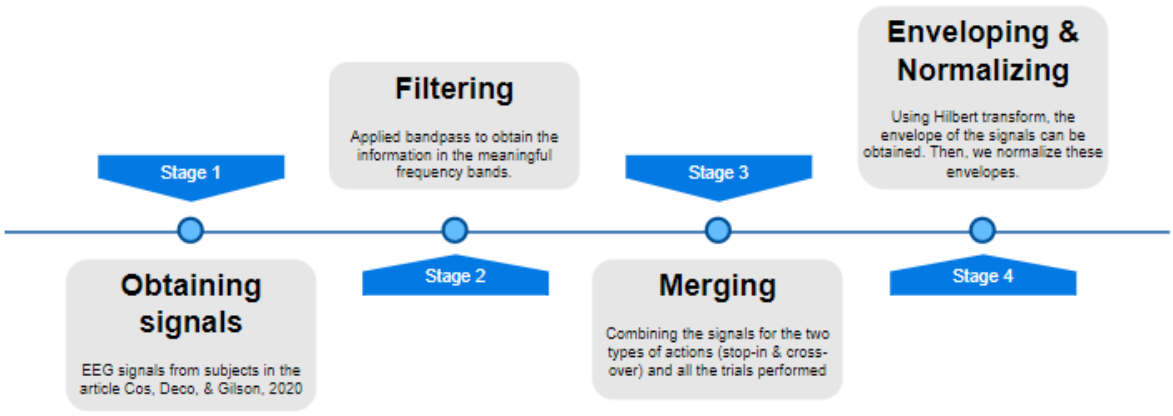

Fig. 1: Phases of processing (Stages 1-4)

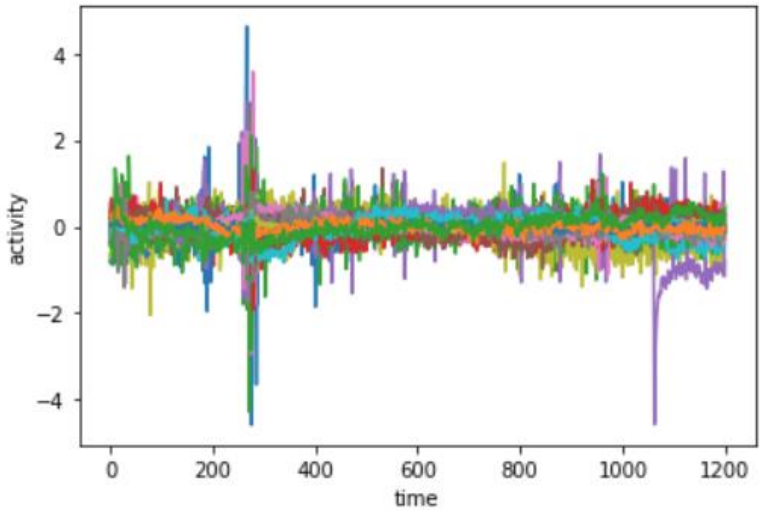

Fig. 2: Original signals, example the first trial, stop-in mode, solo mode and first session of subject 34

It is important to note that human brains operate using a wide range of frequencies, not all of which may be relevant for our analysis. According to EEG literature, the most meaningful frequency ranges in our case are α [8-12 Hz], β [15-32 Hz] and γ [40-80 Hz], since they are associated with visual attention (α-band), bottom-up/ top-down processing (γ-band and β-band, respectively), motor readiness and forward control (β-band), feedback control (γ-band) and hand grip tasks (α-band and β-band coupling). To get the information in these ranges, band-pass filters must be applied. This kind of filters attenuates the signals outside the range of frequencies we have selected while leaving the same the frequencies in that range. The degree of decay of the filter attenuating the outer frequencies is defined by the order of the filter. The higher the order of the filter, the quicker the declivity *(Fig. 3, Fig. 4*).

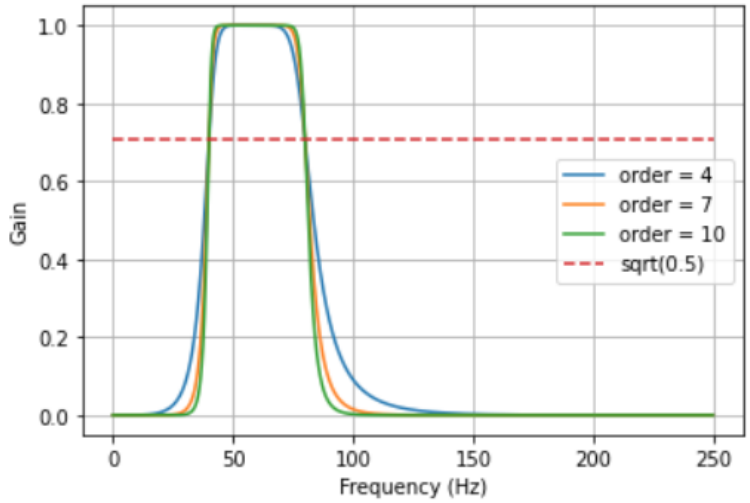

Fig. 3: Example filter orders

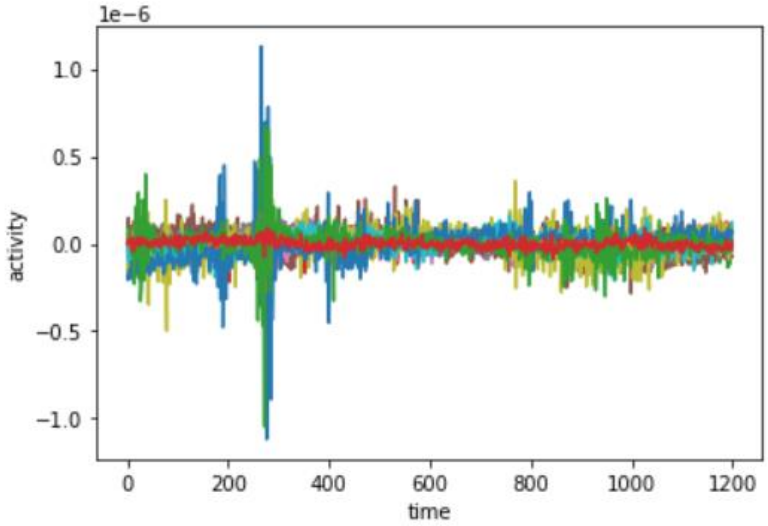

Fig. 4: Filtered signals, same conditions as in Fig. 2

After having filtered to a certain range of frequencies (*Fig.1: Stage 2*), the average signals among "cross-over" and "stop-in" tasks and among all trials and sessions were calculated (*Fig.1: Stage 3, Fig. 5*).

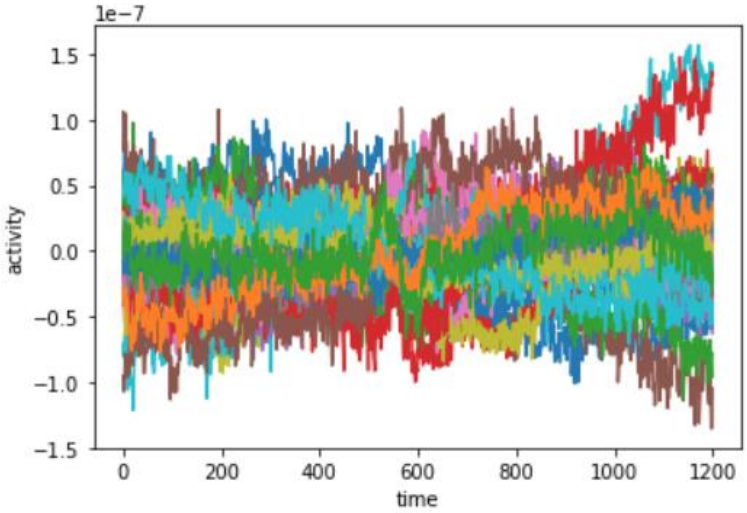

Fig. 5: Merged filtered signals, same conditions as in Fig. 2

There is a final step of data pre-processing before accessing the model, which is obtaining the envelopes of the former signals (*Fig. 1: Stage 4*). Envelopes of signals are the boundary within which the signals are contained (*Fig. 6*).

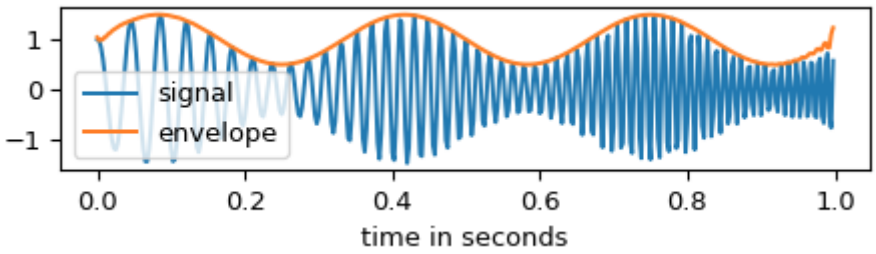

Fig. 6: Example of an envelope

Although envelopes are imaginary curves, they contain some information of signals, as they help generalize the amplitude of these signals. The method used to compute envelopes from the data, which is in time-domain, is the Hilbert transform. This transform can turn a real function into its most "natural" complex extension. It does so by finding a companion function to the real-valued signal such that the real signal can be analytically extended from the real axis to the upper half of the complex plane, that is, it finds a function *H*, called Hilbert transform, so that

$$z(t) = x(t) + jHx(t) \qquad (1)$$

where *z(t)* is the envelope and *x(t)* is the real-valued signal. After that, the envelopes were normalized by subtracting from every source their mean and dividing them by their standard deviation (*Fig. 7*).

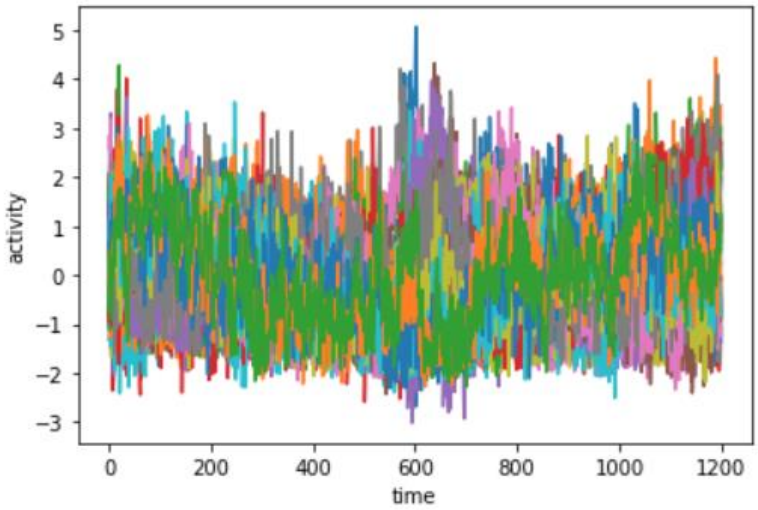

Fig. 7: Normalized signals, same conditions as in Fig. 2

This normalization was needed because later in the model it is required that the activity of each source varies inside the same range of values.

2.2 Introduction to the model

The general idea behind any generative model is to be able to reproduce signals which portrait the dynamics of the original ones. This is done by tuning in some parameters inside the models with the intention of matching the functional connectivity matrices from the model to the ones from the data.

The generative model used in this project is the multivariate Ornstein-Uhlenbeck model (MOU). This model brings balance between simplicity, which ensures tractable analytical calculation, and richness of the generated activities when modulating the parameters. For these reasons, MOU excels at adapting whole-brain cortical activities from a great number of ROIs. Another reason which makes MOU more desirable than other models is that its generated signals present exponential decaying autocovariance, which have similar profiles to the empirical data. (*Fig. 8*)

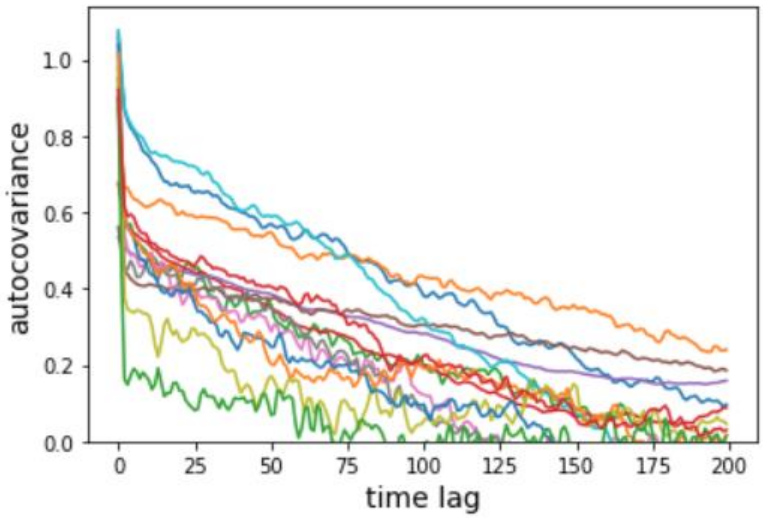

Fig. 8: Autocovariance of the common sources to all subjects for subject 34

2.3 Methodology

Structural connectivity (SC) is defined as the existence of white matter tracts physically interconnecting brain regions. Functional connectivity (FC) is the strength to which activity between a pair of brain regions covaries or correlates over time. In the model, the global pattern of FC arises from the local variability Σ_i (for node i, from 1 to N) that propagates via the network connections EC_{ij} (from nodes i and j, from 1 to N each and i ≠ j).

The general idea of the model is that, starting from the SC of our ROIs, which only considers the relationship between physically connected ROIs and neglects the rest, by iteratively tuning in Σ_i and EC_{ij}, the model spatio-temporal FC, measured by FC0 (covariances without temporal lag) and FCtau (covariance with temporal lag of tau, which value is later discussed) best reproduces the empirical counterpart.

Before starting with the procedure, the value of the temporal lag tau must be extracted. For the fMRI data in *Gilson et al., 2016*, selected tau was 1, since autocovariances were stable and relevant at that point, and only time lags 0, 1 and 2 were computed because signals with higher time lags didn't resemble themselves (less than 0.2 autocovariance) (*Fig. 9*).

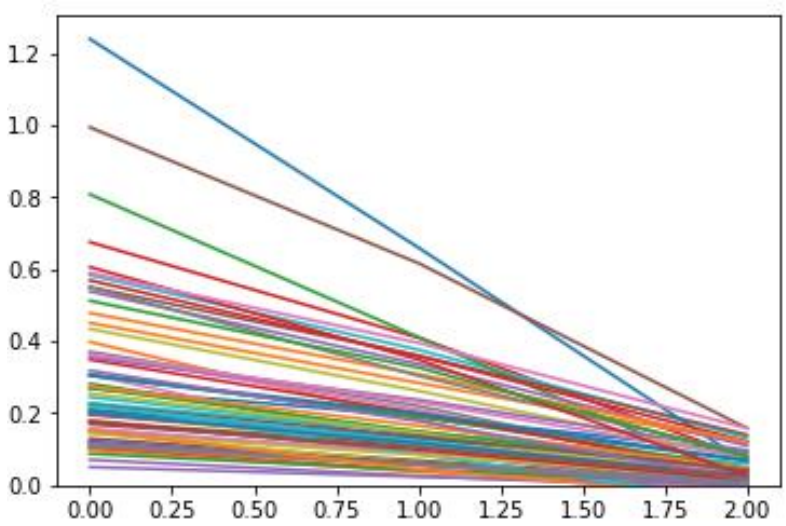

Fig. 9: Autocovariance fMRI example

In our case (*Fig. 8*), tau has been taken as 15 and a total of 200-time lags are calculated, following the former reasoning. This gives sufficient information to gather the model parameters.

After that, the empirical FC0 and FCtau are computed from the normalized envelopes (*Fig. 10: Stage 5*).

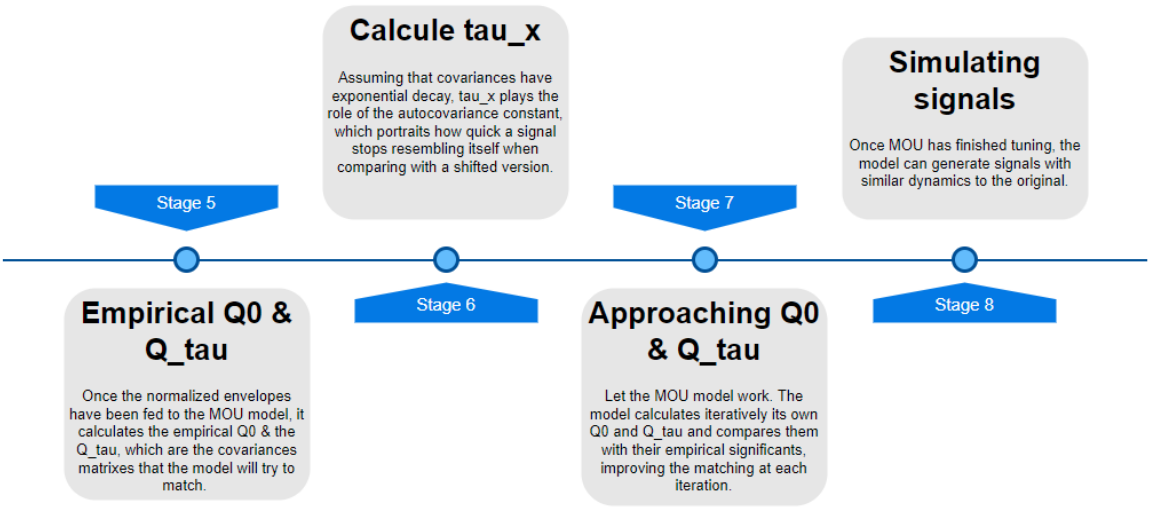

Fig. 10: Phases of processing (stages 5-8)

Let s_i^t be the value from the normalized envelope of source i at time t, then empirical FC0, renamed as $\overline{Q}^0$, and empirical FCtau, renamed as $\overline{Q}^{15}$, can be calculated for each pair (i,j) of nodes as

$$\overline{Q}_{ij}^0 = \frac{1}{T-2}\sum_{t=1}^{T-1} s_i^t * s_j^t$$
$$\overline{Q}_{ij}^{15} = \frac{1}{T-2}\sum_{t=1}^{T-1} s_i^t * s_j^{t+15} \qquad (2)$$

The activities of nodes in the multivariate Ornstein-Uhlenbeck process exponentially decay with a time constant and they evolve depending on the activity of other population, following the next formula:

$$dx_i = \left(\frac{-x_i}{\tau_x} + \sum_{j \neq i} C_{ij}x_j\right)dt + dB_i \qquad (3)$$

where τ_x time constant, C_{ij} network effective connectivity (the aforementioned EC_{ij}) and dB_i Wiener process (or Brownian motion) with covariance matrix Σ_i.

Due to the simplicity of the model, it is possible to have analytic estimations of the model covariances, defined as Q_{ij}^0 and Q_{ij}^{15}, which reproduce $\overline{Q}_{ij}^0$ and $\overline{Q}_{ij}^{15}$, respectively. Let J_{ij} be the Jacobian of the dynamical system, calculated as

$$J_{ij} = \frac{-\delta_{ij}}{\tau_x} + C_{ij}\ , \qquad (4)$$

where δ_{ij} is the Kronecker delta ($\delta_{ij} = 1\ if\ i = j, \delta_{ij} = 0\ if\ i \neq j$), then Q_{ij}^0 can be obtained by solving the Lyapunov equation

$$JQ^0 + Q^0J^T + \Sigma\ , \qquad (5)$$

and Q_{ij}^{15} is then given by

$$Q^{15} = Q^0 e^{15J^T}\ , \qquad (6)$$

where e^{J^T} is a matrix exponential of transposed J. To do this, it is required to know the parameters τ, C and Σ.

The first parameter calculated is τ (*Fig. 10: Stage 6*). It helps "calibrate" the model before the optimization steps. It is calculated as:

$$\tau_x = \frac{1}{N}\sum_{i=1}^{N}\frac{1}{\log(\overline{Q}_{ii}^{0}) - \log(\overline{Q}_{ii}^{15})} \tag{7}$$

Note that because it only depends on $\overline{Q}^0$ and $\overline{Q}^{15}$, which are immutable, its value doesn't change during the optimization process.

After τ_x value has been set, an iterating optimization takes place (*Fig. 10: Stage 7*). The idea is that after each iteration Q^0 and Q^{15} resemble more $\overline{Q}^0$ and $\overline{Q}^{15}$, respectively, or what is the same, that the model error E defined as

$$E = \frac{1}{2}\frac{\sum_{i,j}(\Delta Q_{ij}^{0})}{\sum_{i,j}(\overline{Q}_{ij}^{0})} + \frac{1}{2}\frac{\sum_{i,j}(\Delta Q_{ij}^{15})}{\sum_{i,j}(\overline{Q}_{ij}^{15})} \tag{8}$$

where $\Delta Q^0 = \overline{Q}^0 - Q^0$ and $\Delta Q^{15} = \overline{Q}^{15} - Q^{15}$, gets progressively smaller. To achieve this, the algorithm starts with $C = 0$ and Σ homogeneous and calculates the Q^0 and Q^{15} for that iteration. Using them, it calculates that iteration model error and updates the Jacobian by

$$\Delta J^T = (Q^0)^{-1}[\Delta Q^0 + \Delta Q^{15} e^{J^T}] \tag{9}$$

which decreases the model error E of the next step, similar to a gradient descent. The update in C is

$$\Delta C = \eta_C \Delta J \tag{10}$$

for the connections allowed by the SC; otherwise forced at 0. The update in Σ is

$$\Delta \Sigma = -\eta_\Sigma (J\Delta Q^0 + \Delta Q^0 J^T) \tag{11}$$

for elements in the diagonal, otherwise forced at 0. The values of η_C and η_Σ have been left untouched with respect to *Gilson et al., 2016*, being $\eta_C = 0.0005$ and $\eta_\Sigma = 0.05$.

Once the values of the parameters τ, C and Σ been found, the model is able to generate signals with similar dynamics to the normalized envelopes. This is possible by using the tuned-in parameters τ, C and Σ and the formula in (*3*). To remove the effect of the initial conditions, the results of the process in a starting interval of time T0 are not recorded (*Fig. 11*).

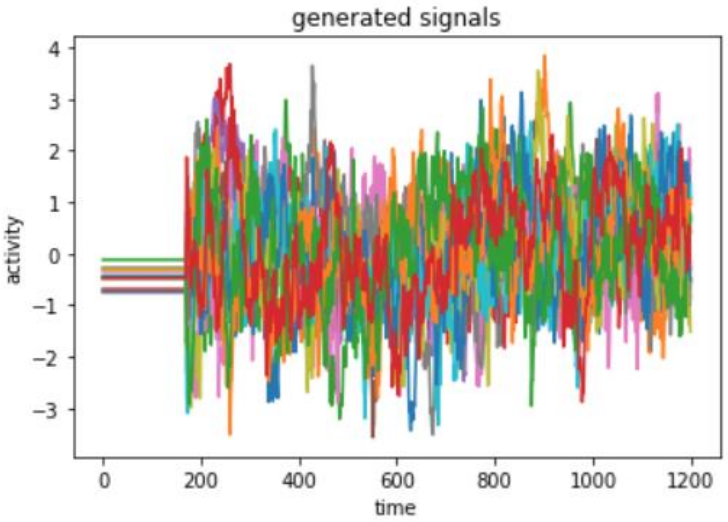

Fig. 11: Signals generated by the model for same conditions as in Fig. 2

It is important to note that, since normalized envelopes were used to create $\overline{Q}^0$ and $\overline{Q}^{15}$, MOU cannot generate similar signals to those envelopes like it normally could if they were regular signals. It does still provide similar dynamics and the effective connectivity is computed correctly.

2.4 Classification of motivations

The effective connectivity parameter C which gets tuned in by the MOU model optimisation, explained in previous stages, can be used to train a classifier the goal of which is distinguishing the three motivational levels solo, easy and hard. In order to feed the classifier, C is to be calculated for every subject, motivation, band and trial, which means optimising the MOU model for the envelopes obtained for each of these circumstances. After that, the zscore of each C are computed. The zscore provides the number of standard deviations a sample is shifted with respect to the mean of the group of samples. The formula to calculate the zscore z of a sample x is

$$z = (x - \mu)/\sigma \qquad (12)$$

, where μ and σ are the mean and standard deviation of the group of samples, respectively.

In this project, two classifiers are trained and tested with these zscores, which are multiple linear regression (MLR) and 1-nearest neighbour (1NN). The results obtained by the classifiers using this connectivity method are compared with other connectivities, like functional connectivity (FC) and partial correlations (PC), and with the corresponding chance level, which is the probability of obtaining these results by chance (in our case, one out of three because there are three motivational levels).

3 RESULTS

As stated previously in the data treatment section, source spaces had a dimension from 40 to 50 sources after eliminating noisy and artefactual sources, but the remaining sources were not the same for all subjects. For this reason, it is interesting to separate the information into subject specific results and average subject results.

3.1 Single-subject results

In this section, the goal is to obtain how the band the signals are being filtered by and the motivational level affects the outcome of the fitting and the resemblance between empirical and model connectivity. Also, it is meaningful to see how the previous outcomes vary if instead of all the sources from the source space only common sources to all subjects are being considered. To simplify this section, only the results for a subject will be presented here, while other relevant subjects are presented at the annex. For subject 25, we obtained the following covariances matrices when considering all sources (see on next page).

Frequency Bands	Motivational levels: SOLO	Motivational levels: EASY	Motivational levels: HARD
α	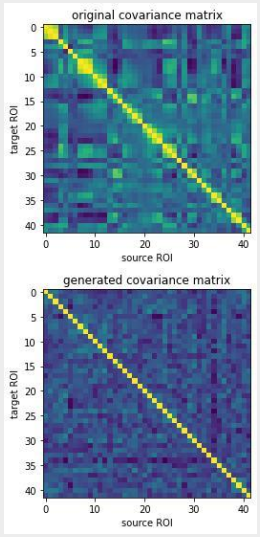	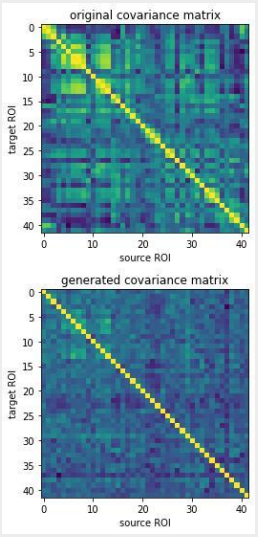	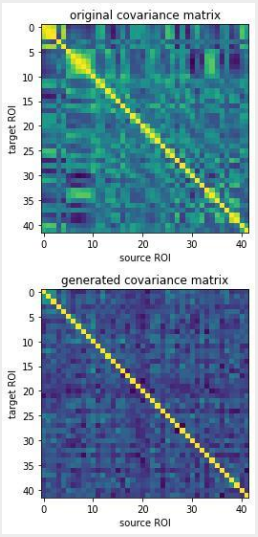
β	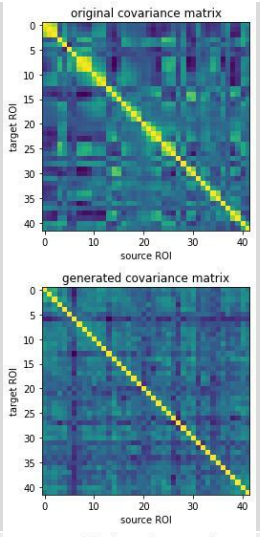	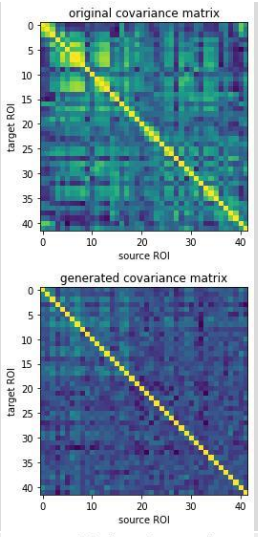	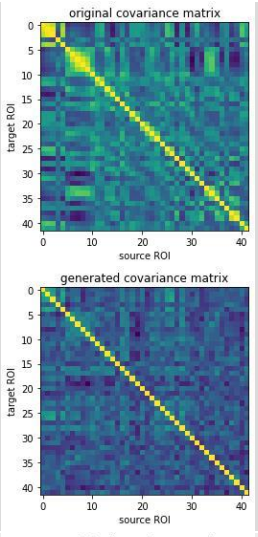
γ	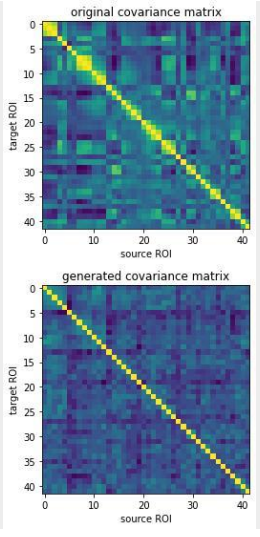	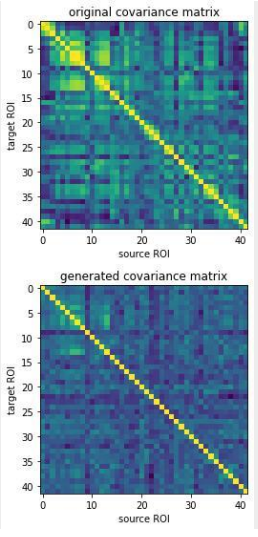	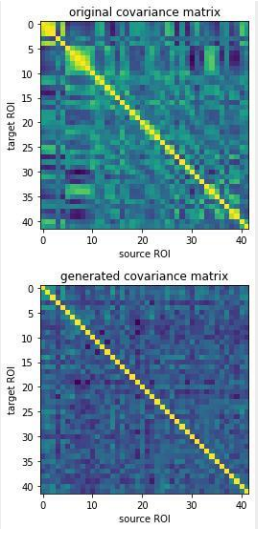

The correlations between these pairs of matrices are:

		Motivational levels		
		SOLO	EASY	HARD
Frequency Bands	α	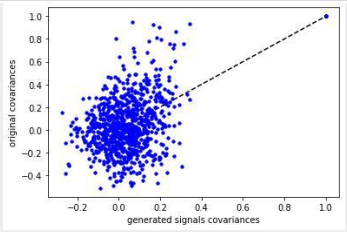 Correlation: 0.5633	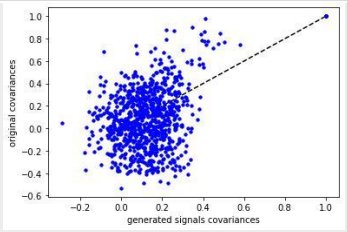 Correlation: 0.5065	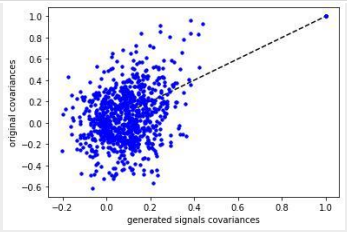 Correlation: 0.5408
	β	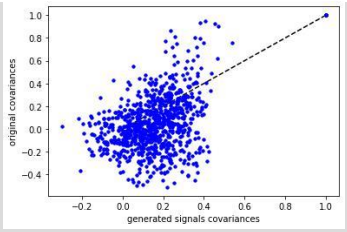 Correlation: 0.5714	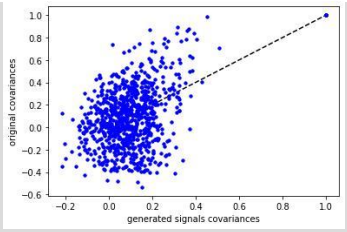 Correlation: 0.5465	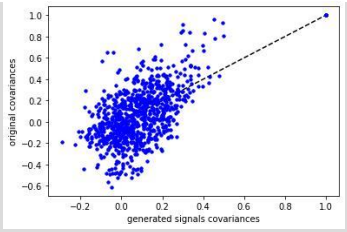 Correlation: 0.6842
	γ	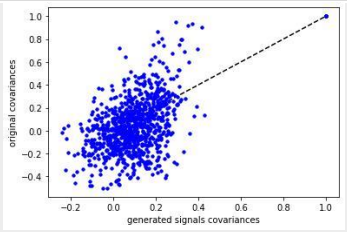 Correlation: 0.6401	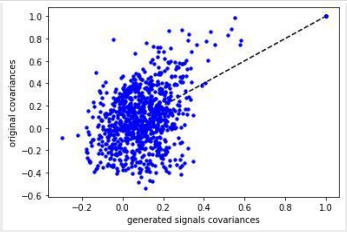 Correlation: 0.5609	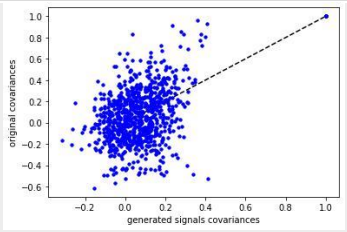 Correlation: 0.5643

The average correlation between covariance matrices is 0.5722.

When only considering the common sources to all subjects for the same subject analysed previously, the resulting model covariances matrices resemble the empirical ones significantly better (see on next page).

Frequency Bands	Motivational levels: SOLO	EASY	HARD
α	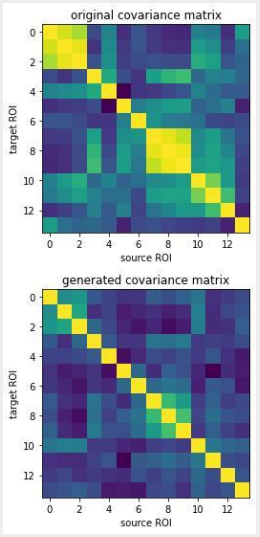	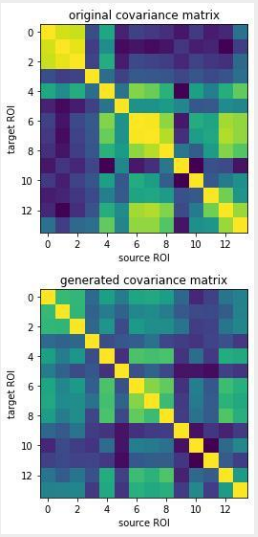	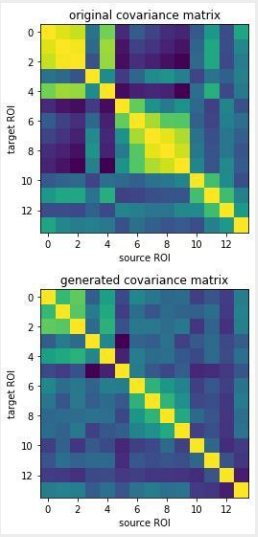
β	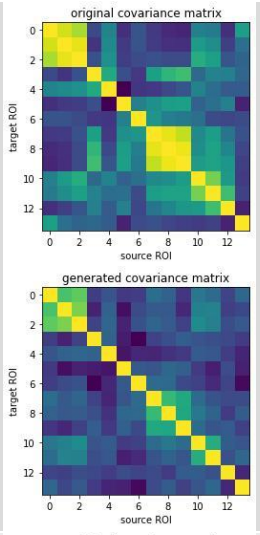	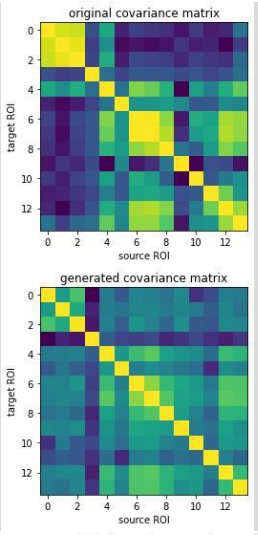	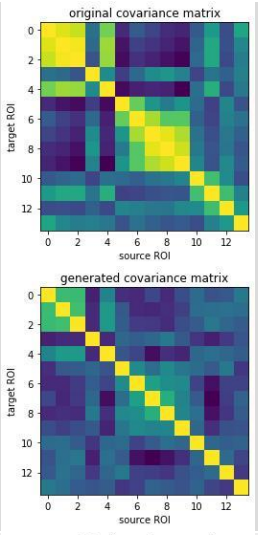
γ	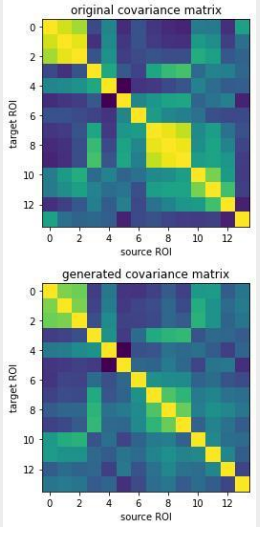	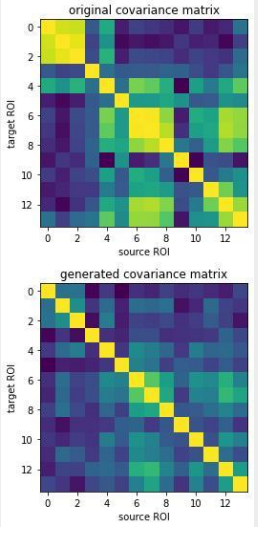	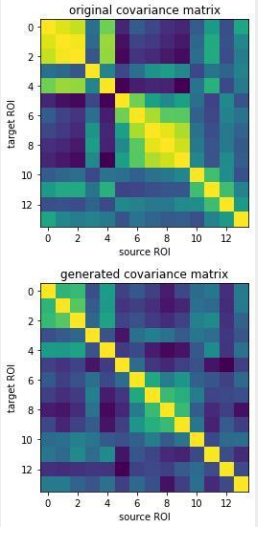

The correlations between these closer-looking pairs of matrices are:

Frequency Bands	Motivational levels: SOLO	EASY	HARD
α	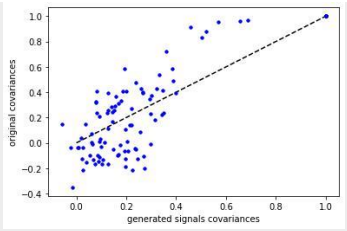 Correlation: 0.8175	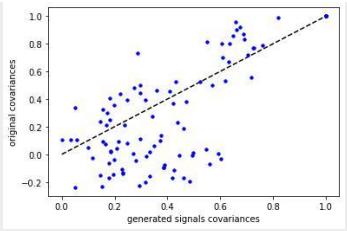 Correlation: 0.7297	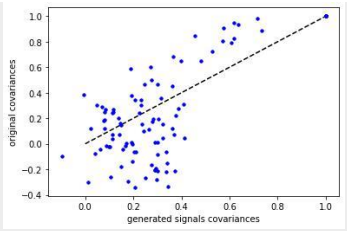 Correlation: 0.7344
β	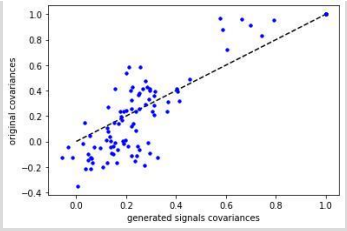 Correlation: 0.8664	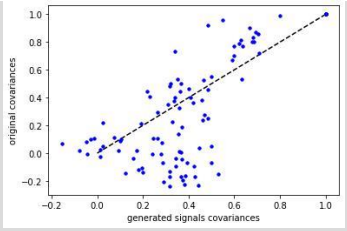 Correlation: 0.7296	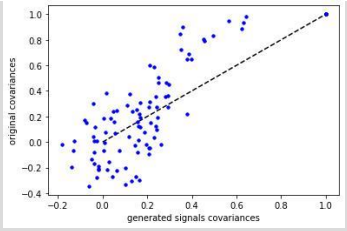 Correlation: 0.8255
γ	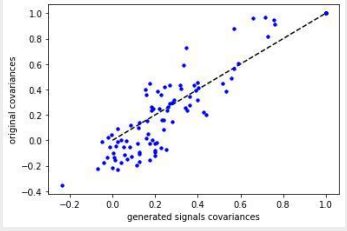 Correlation: 0.9111	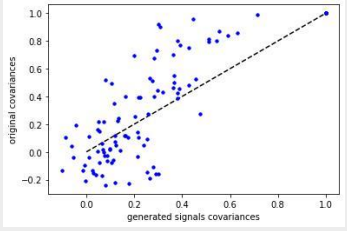 Correlation: 0.8000	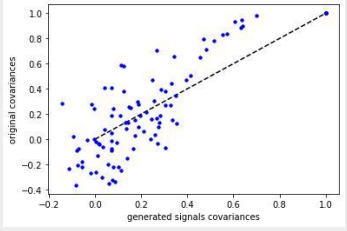 Correlation: 0.8450

The average correlation between covariance matrices is 0.8065.

3.2 Across-subjects results

In this section, the goal is to show the average model error and correlation of all subjects for the different motivation states and frequency bands. These results are represented being 0 the solo mode, 1 the easy mode and 2 the hard mode (see on next page).

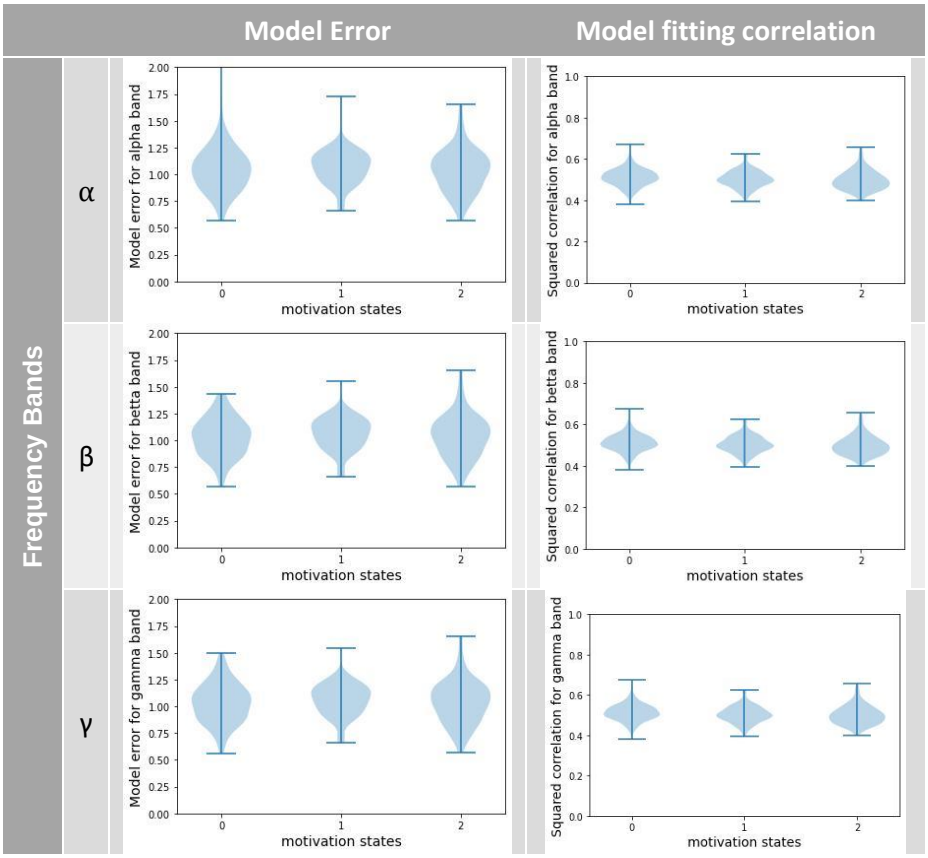

Note: Model fitting correlation refers to the correlation between the empirical connectivity $\overline{Q}^0$ and $\overline{Q}^{15}$ and the model connectivity Q^0 and Q^{15}, which is not to the same as the previous section correlation between covariance matrices of signals.

3.3 Classification

Accuracy of the classifiers for subject 25's motivational levels are shown next, comparing the usage of all sources with the usage of only the common sources across subjects, side by side with blue colour representing MLR and orange 1NN (see on next page).

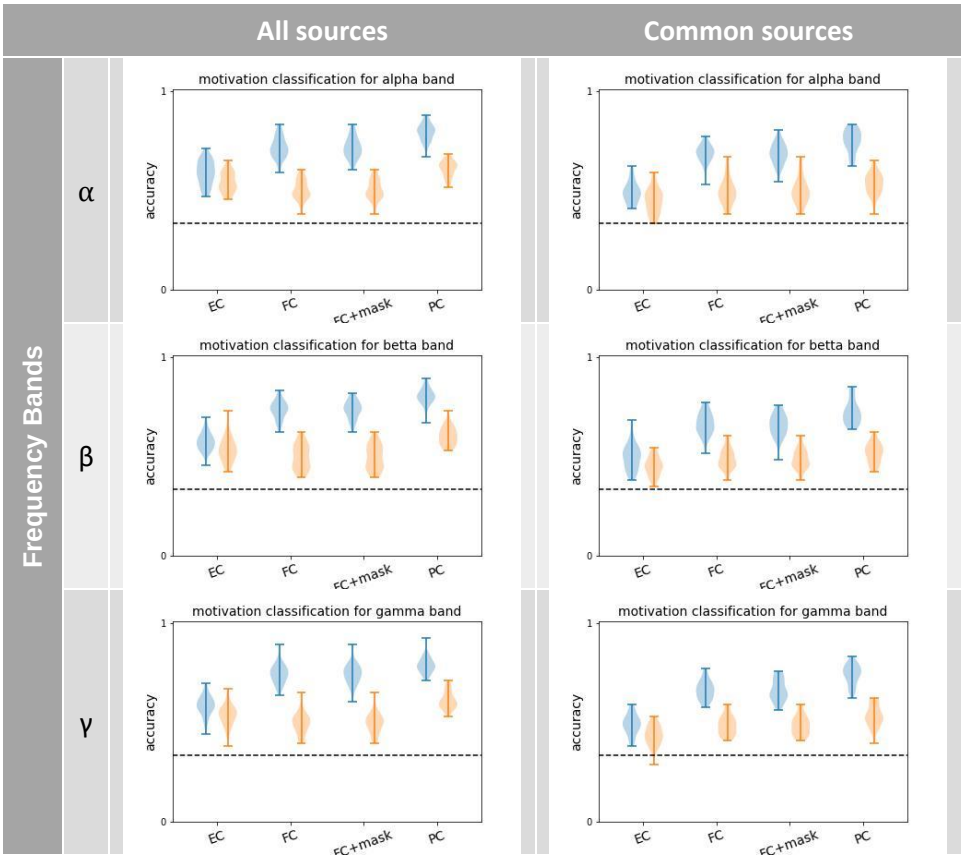

The previous accuracies for MLR and 1NN resulted into the following confusion matrices.

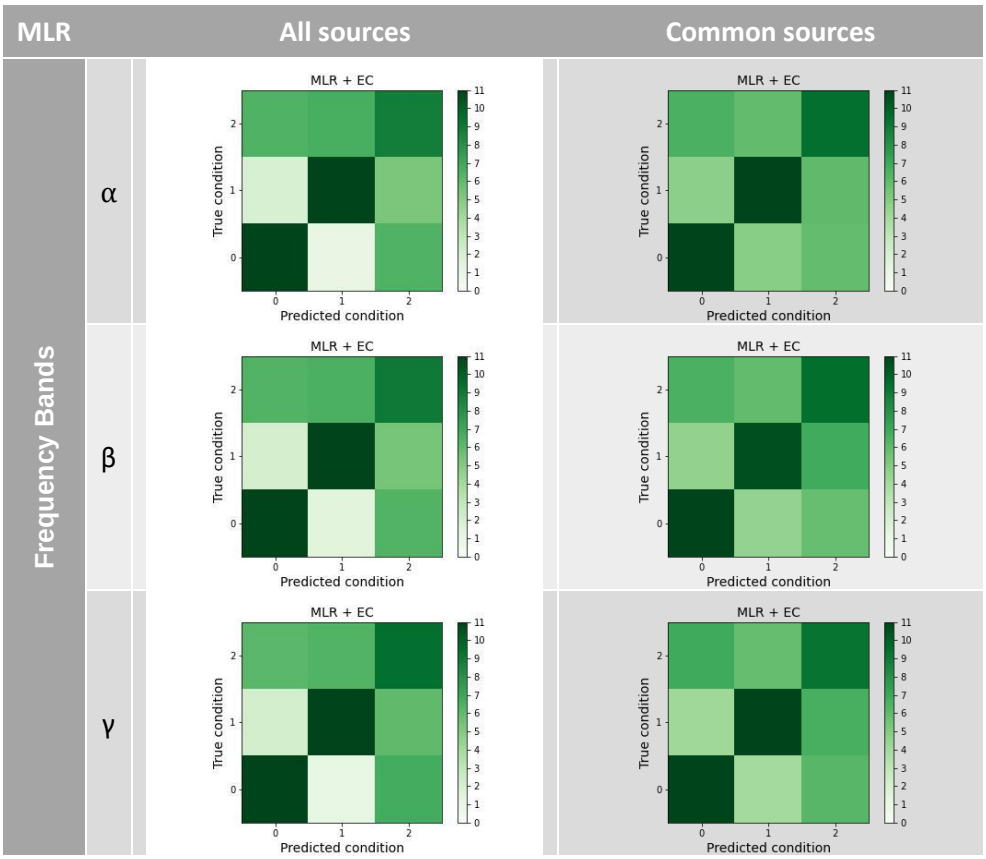

1NN		All sources	Common sources
Frequency Bands	α	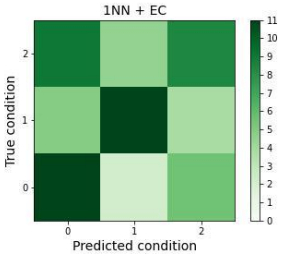	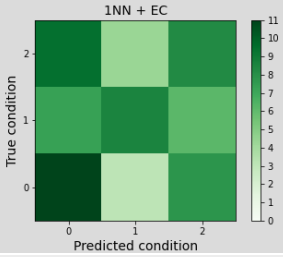
	β	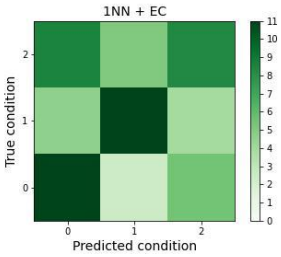	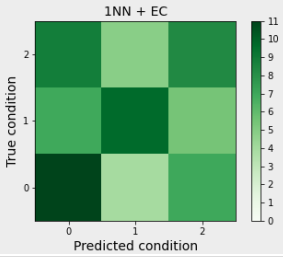
	γ	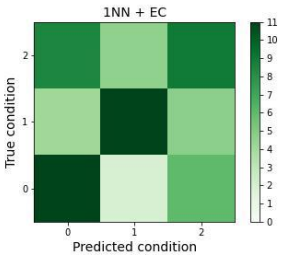	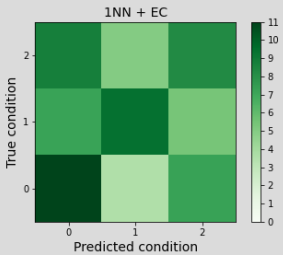

4 CONCLUSIONS AND FUTURE WORK

The results show that it is possible for the multivariate Ornstein-Uhlenbeck to replicate the EEG dynamics for each subjects up to 60-65%, increasing when only considering the common sources which remained after filtering the source spaces for all subjects up to 80-85%. This could be because common sources are better at "tracking" each other activities, meaning they have an increased effect in each other. By considering only common sources some sources the activity of which may not be affected by others and not be affected by the arousal of subjects either, which would be harder to define using MOU formula (3), may have been excluded.

It seems that using the zscores of the effective connectivity matrices obtained from the parameter C of the MOU to train/test a 1NN classifier brings meaningful results, having higher accuracy than chance level for all subjects, but not as good as the other connectivity methods. This aftermath is even more pronounced in the MLR classifier, where accuracies for zscores are all above chance level but way lower than other connectivity metrics. In contrast with previous paragraph where better results were generated for common sources, the accuracies of classification using EC were closer to the accuracies of other metrics when considering all sources for each subject, being even better in some cases.

Remarkably, the results in *Cos et al., 2022* proved that classifiers obtained higher accuracies when filtering by the gamma band for functional connectivity and partial correlations, fact that is not presented in these results and should be looked into.

Another possible improvement could arise by better selecting the time-shift of FCtau and number of time lags calculated discussed at section 2.3, personalizing them for every subject's autocovariances.

In the original MOU model prepared for fMRI data in *Gilson et al., 2016*, signals feed to the model were centred by removing their means, but the envelopes in this project were so reduced in amplitude after filtering by the bands that a stronger normalization had to be applied (otherwise the MOU model attempted to match extremely small covariance matrices and that raised high model errors and some classifiers didn't even work). That being said, dividing the envelopes by their standard deviation may not have been the better practice and other alternatives should be investigated.

5 REFERENCES

Cos, Deco, & Gilson (2022). "THE INFLUENCE OF INTRINSIC MOTIVATION ON DECISIONS BETWEEN ACTIONS." , under review at Scientific Reports.

Gilson et al. (2016). "Estimation of Directed Effective Connectivity from fMRI Functional Connectivity Hints at Asymmetries of Cortical Connectome."

Gilson et al. (2020). "Model-based whole-brain effective connectivity to study distributed cognition in health and disease."

Pallarés et al. (2018). "Extracting orthogonal subject- and condition-specific signatures from fMRI data using whole-brain effective connectivity."

NHS (2022). *Electroencephalogram (EEG).* Retrieved on April 1, 2022 from https://www.nhs.uk/conditions/electroencephalogram/

IMOTIONS (August 23, 2019). "Top 3 Devices for Monitoring and Measuring Brain Activity". Retrieved on April 5, 2022 from https://imotions.com/blog/top-3-devices-measuring-brain-activity/

Yanli, Y. (March 31, 2017). "A Signal Theoretic Approach for Envelope Analysis of Real-Valued Signals". Retrieved on April 30, 2022 from https://ieeexplore.ieee.org/stamp/stamp.jsp?arnumber=7891054

QUORA (2018). "Why should the shape of the envelope be the same as that of the modulating signal?". Retrieved on April 30, 2022 from https://www.quora.com/Why-should-the-shape-of-the-envelope-be-the-same-as-that-of-the-modulating-signal

Viswanathan, M. (April 20, 2017). "Understanding Analytic Signal and Hilbert Transform". Retrieved on May 15, 2022 from https://www.gaussianwaves.com/2017/04/analytic-signal-hilbert-transform-and-fft/

MATHEMATICS (2016). "Intuition behind Fourier and Hilbert transform". Retrieved on May 15, 2022 from https://math.stackexchange.com/questions/1717578/intuition-behind-fourier-and-hilbert-transform

IMOTIONS (July 12, 2019). "EEG vs. MRI vs. fMRI – What are the Differences?". Retrieved on April 1, 2022 from https://imotions.com/blog/eeg-vs-mri-vs-fmri-differences/

6 ANNEX

Results for subject 31 (remarkable for having good results in all aspects).

		Motivational levels		
		SOLO	EASY	HARD
Frequency Bands	α	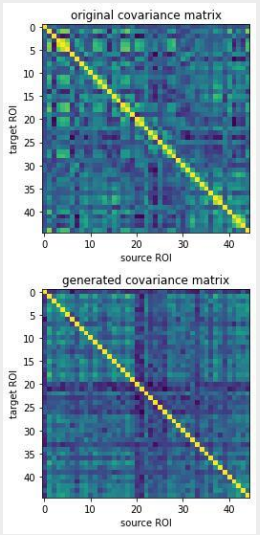	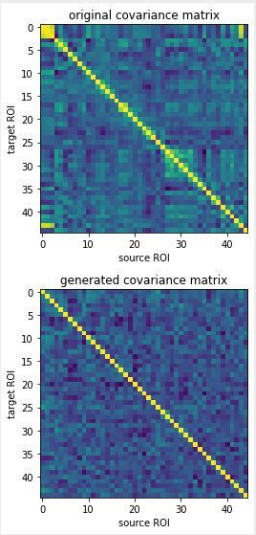	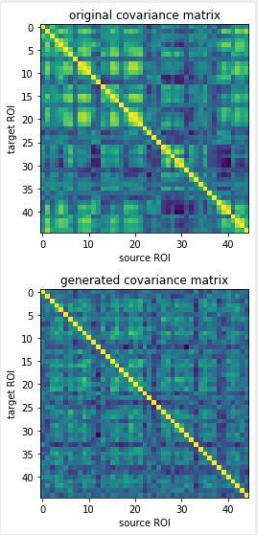
	β	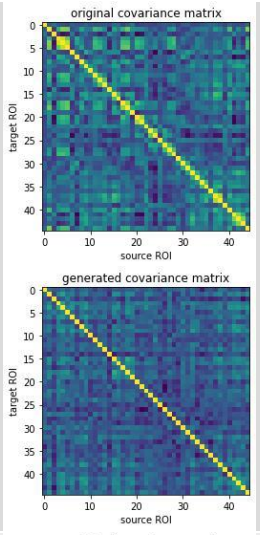	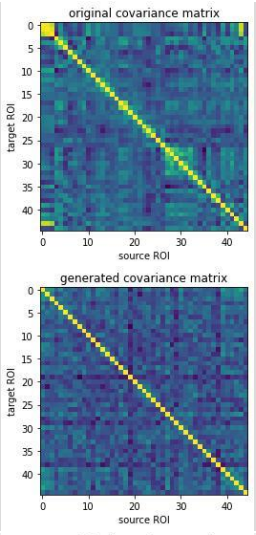	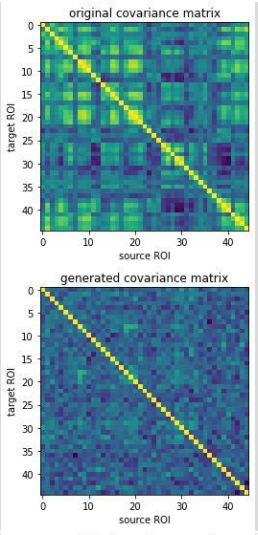
	γ	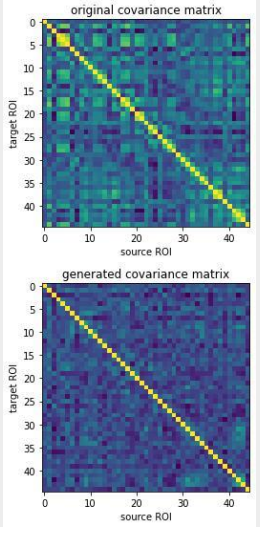	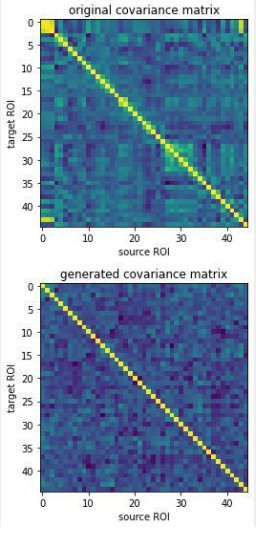	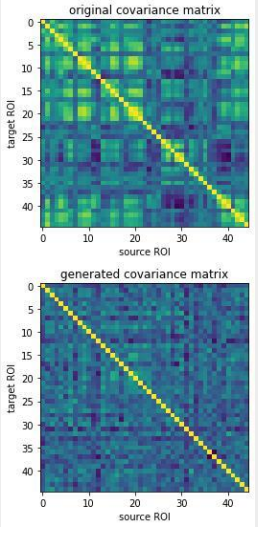

Frequency Bands		Motivational levels		
		SOLO	EASY	HARD
	α	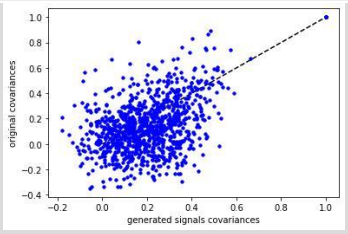 Correlation: 0.5800	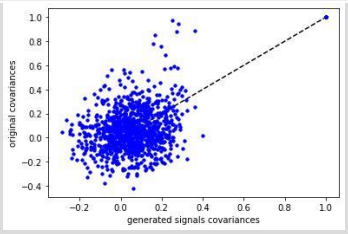 Correlation: 0.5906	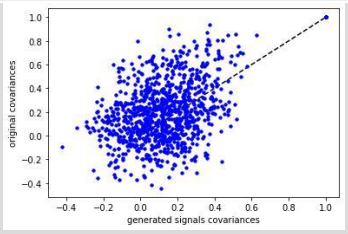 Correlation: 0.5016
	β	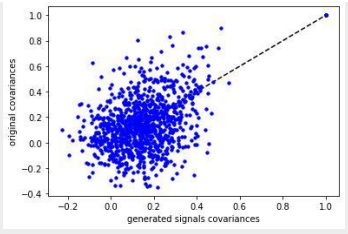 Correlation: 0.5692	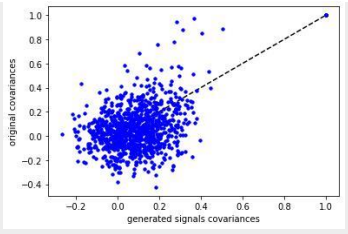 Correlation: 0.6081	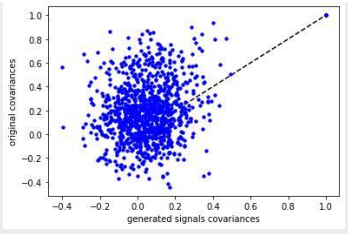 Correlation: 0.4092
	γ	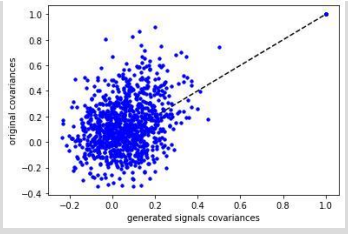 Correlation: 0.5620	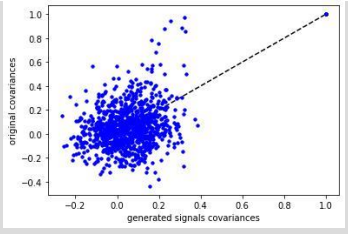 Correlation: 0.5986	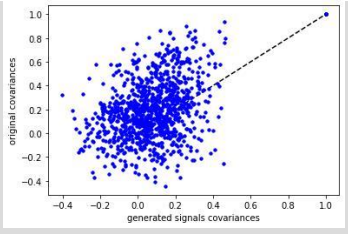 Correlation: 0.5043

The average correlation between covariance matrices is 0.5470.

Frequency Bands	Motivational levels: SOLO	Motivational levels: EASY	Motivational levels: HARD
α	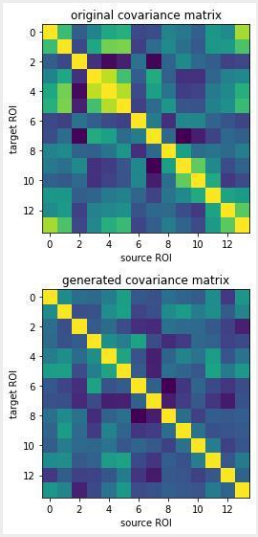	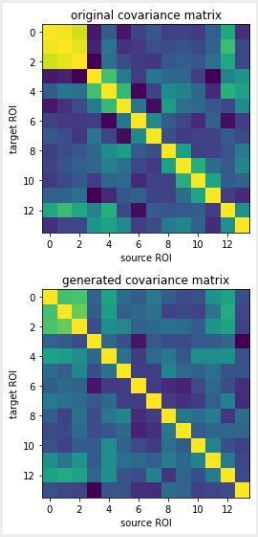	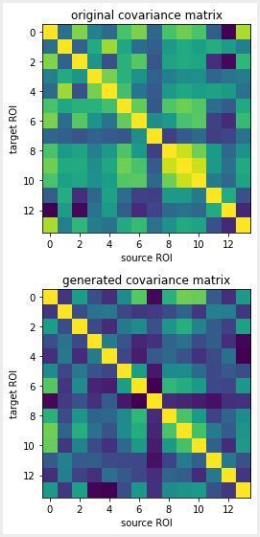
β	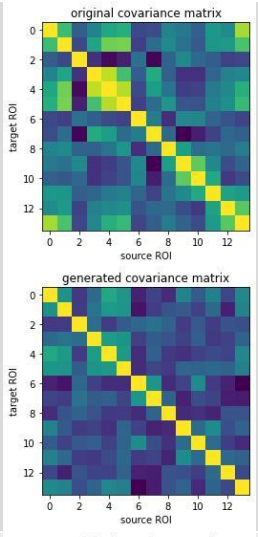	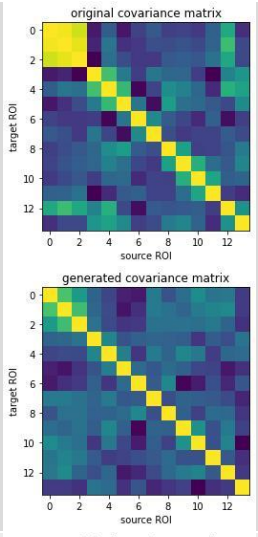	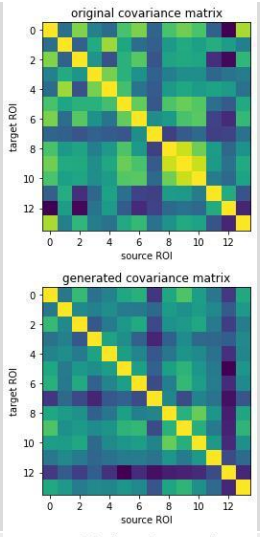
γ	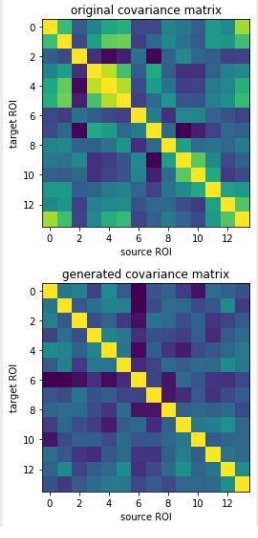	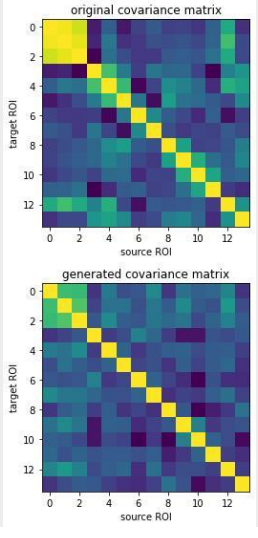	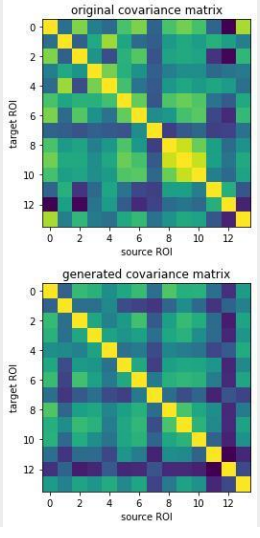

Frequency Bands	Motivational levels: SOLO	EASY	HARD
α	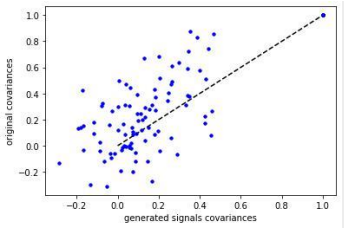	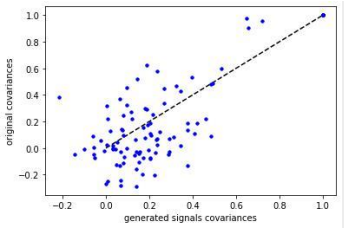	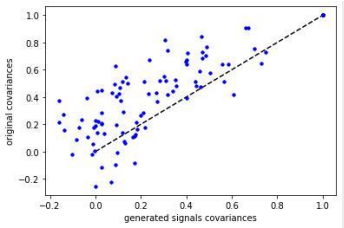
	Correlation: 0.7501	Correlation: 0.7770	Correlation: 0.8115
β	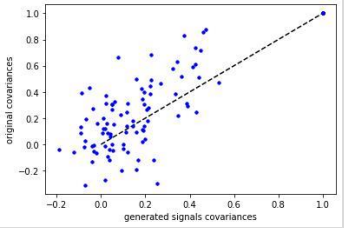	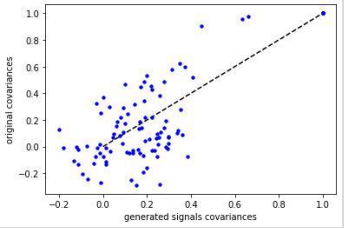	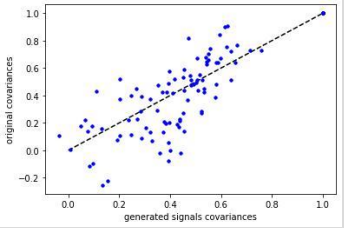
	Correlation: 0.7883	Correlation: 0.7760	Correlation: 0.8080
γ	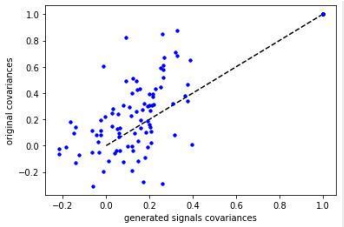	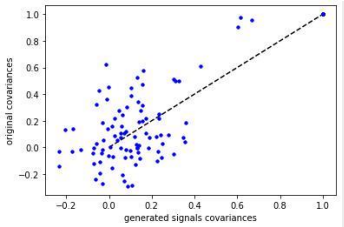	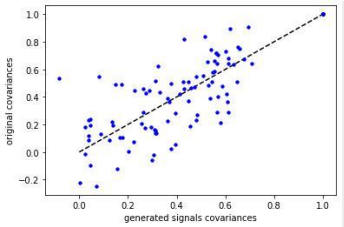
	Correlation: 0.7353	Correlation: 0.7721	Correlation: 0.7784

The average correlation between covariance matrices is 0.7774.

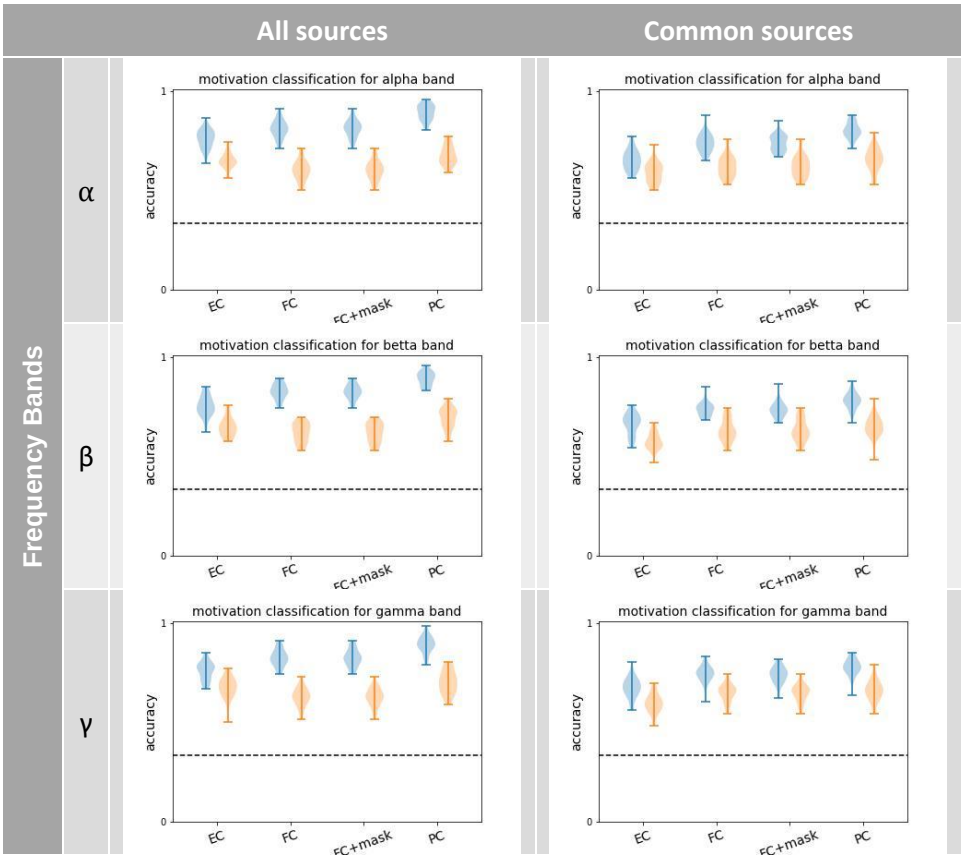
All sources
Common sources
Frequency Bands
α
β
γ
motivation classification for alpha band
motivation classification for betta band
motivation classification for gamma band
accuracy
EC
FC
FC+mask
PC

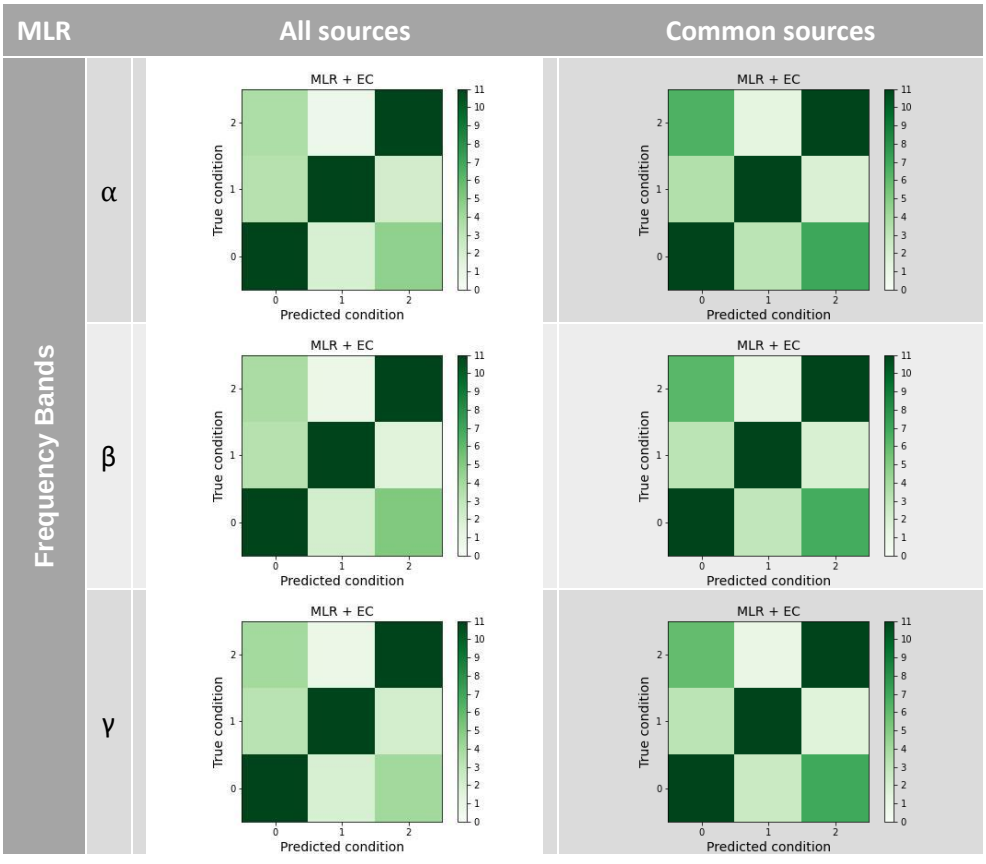
MLR
All sources
Common sources
Frequency Bands
α
β
γ
MLR + EC
True condition
Predicted condition

1NN		All sources	Common sources
Frequency Bands	α	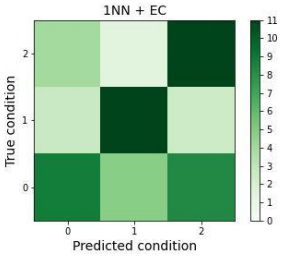	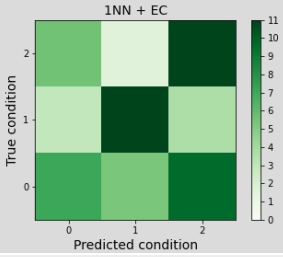
	β	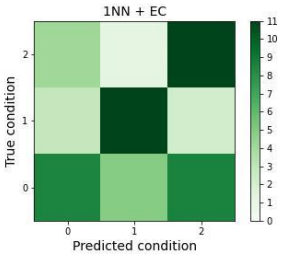	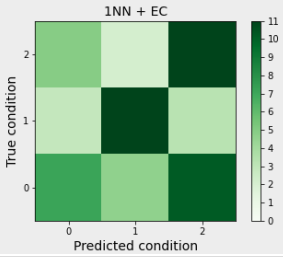
	γ	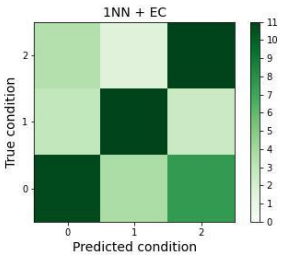	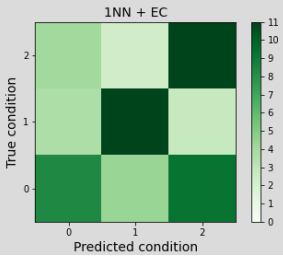

Results for subject 34 (remarkable for having good fitting and being able to recreate the dynamics of the activity, but having accuracy at classifying near to chance level for all connectivities metrics)

		Motivational levels		
		SOLO	EASY	HARD
Frequency Bands	α	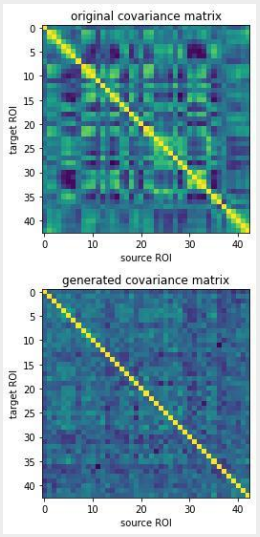	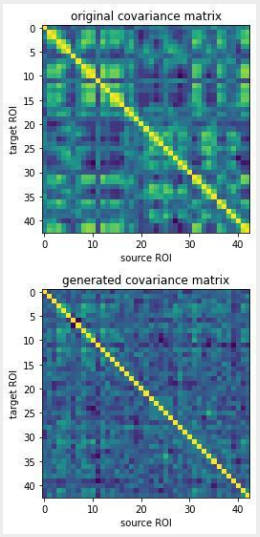	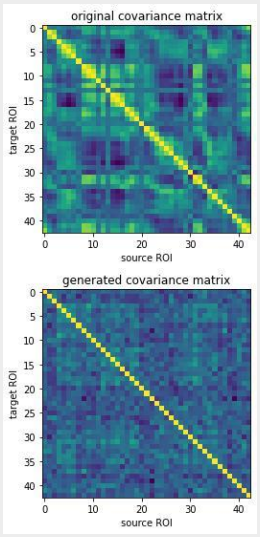
	β	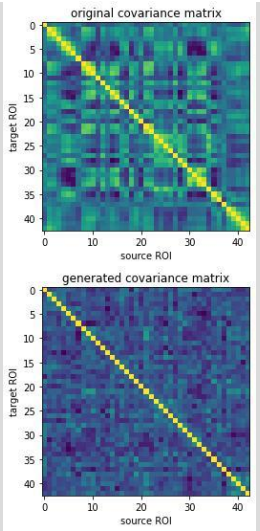	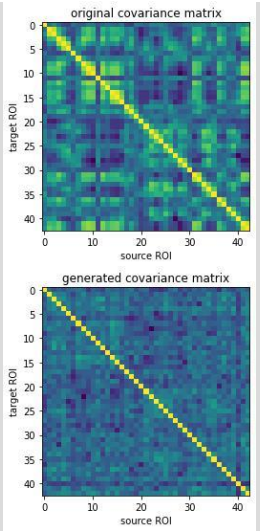	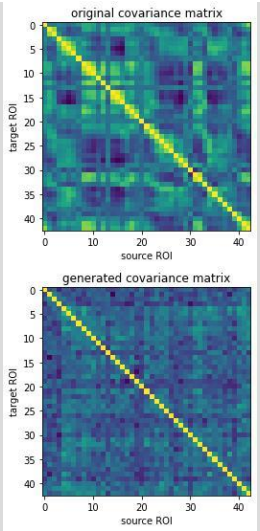
	γ	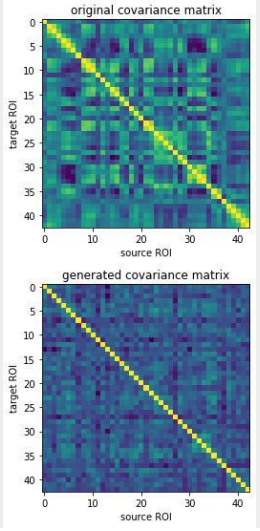	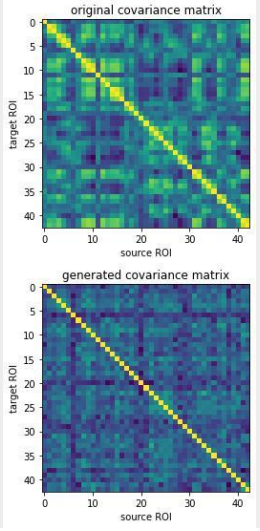	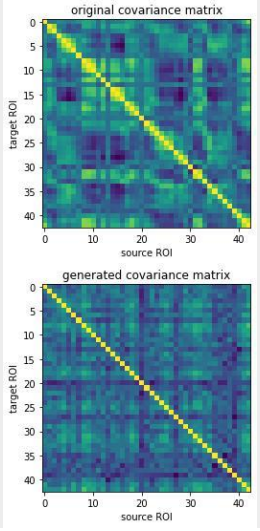

Frequency Bands	Motivational levels: SOLO	Motivational levels: EASY	Motivational levels: HARD
α	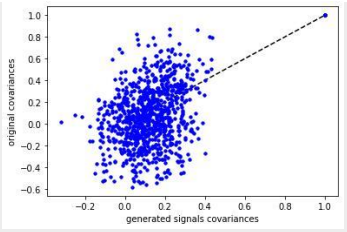 Correlation: 0.5120	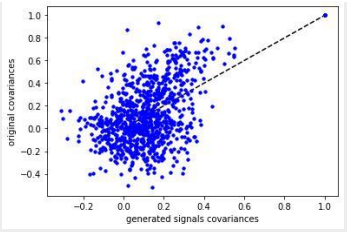 Correlation: 0.5718	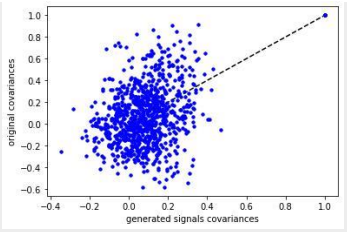 Correlation: 0.5018
β	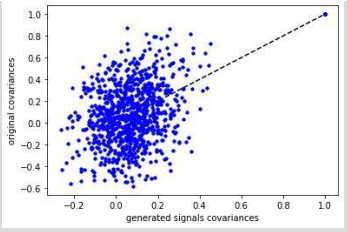 Correlation: 0.5016	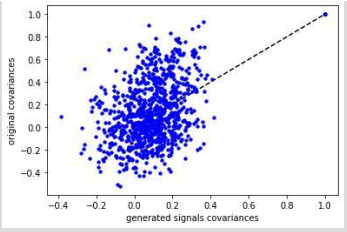 Correlation: 0.5258	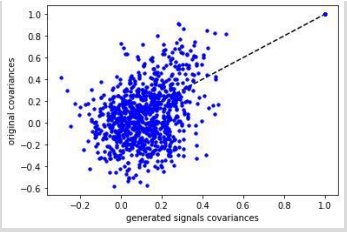 Correlation: 0.5424
γ	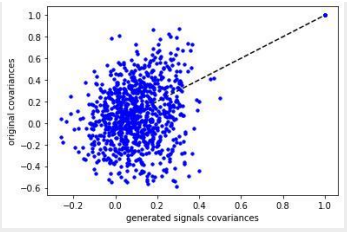 Correlation: 0.4471	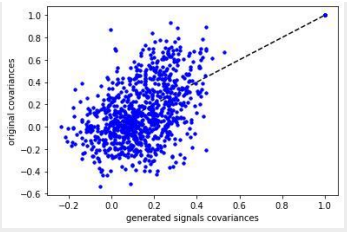 Correlation: 0.5814	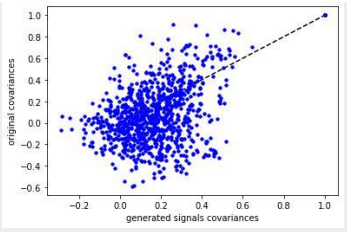 Correlation: 0.5135

The average correlation between covariance matrices is 0.5219.

Frequency Bands	Motivational levels: SOLO	Motivational levels: EASY	Motivational levels: HARD
α	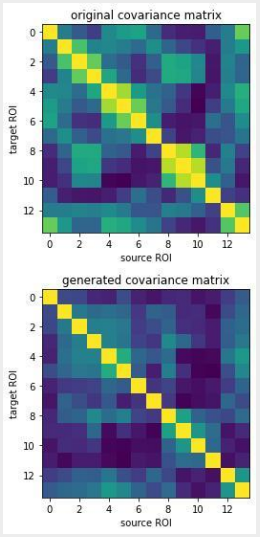	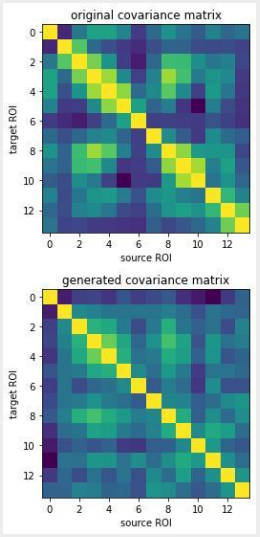	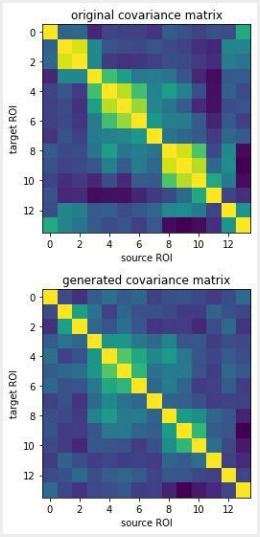
β	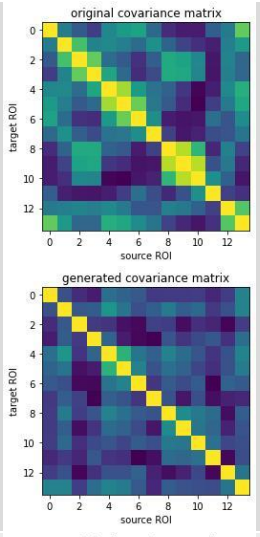	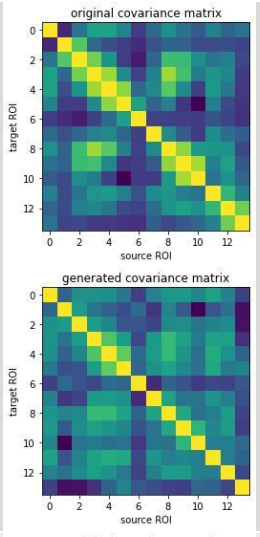	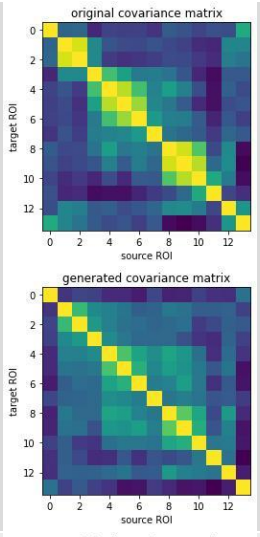
γ	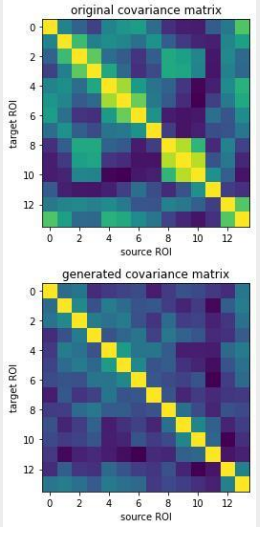	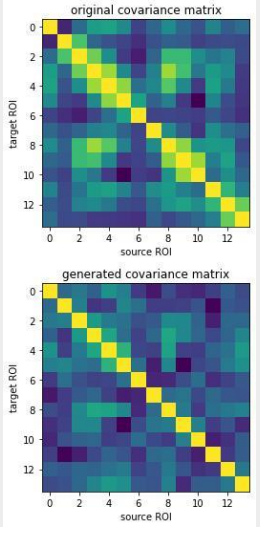	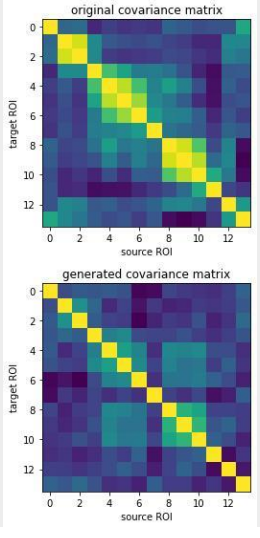

Frequency Bands	Motivational levels: SOLO	EASY	HARD
α	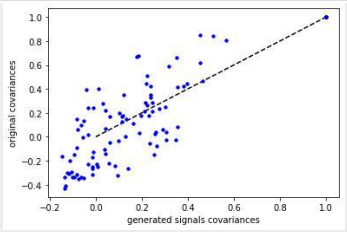 Correlation: 0.8300	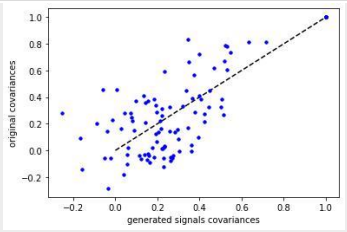 Correlation: 0.7521	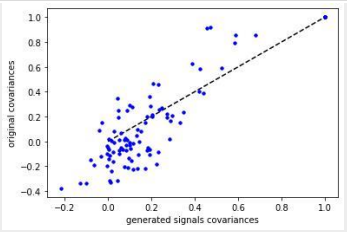 Correlation: 0.8858
β	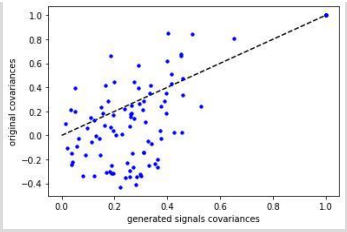 Correlation: 0.6935	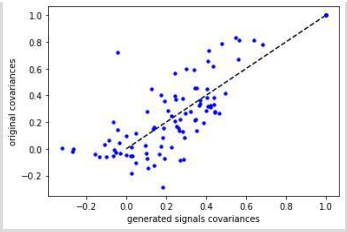 Correlation: 0.8202	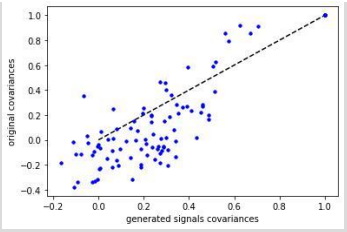 Correlation: 0.8528
γ	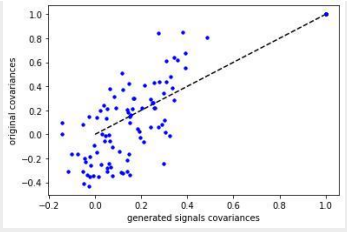 Correlation: 0.8004	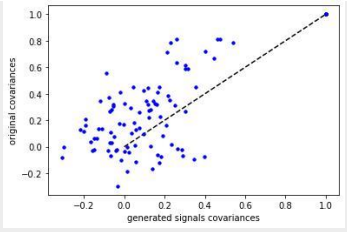 Correlation: 0.7322	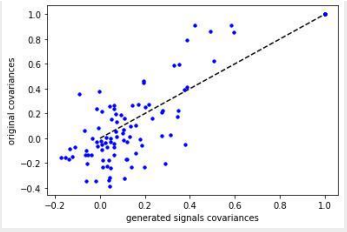 Correlation: 0.8318

The average correlation between covariance matrices is 0.7998.

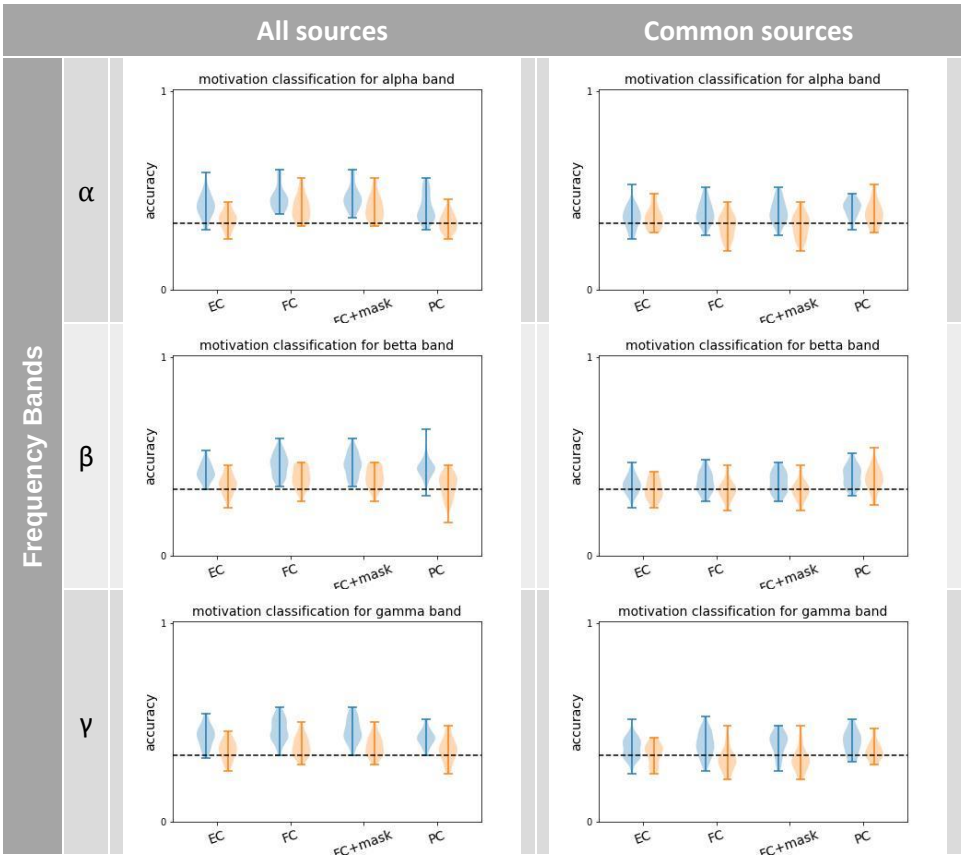
All sources
Common sources
Frequency Bands
α
β
γ
motivation classification for alpha band
motivation classification for betta band
motivation classification for gamma band
accuracy
EC
FC
FC+mask
PC

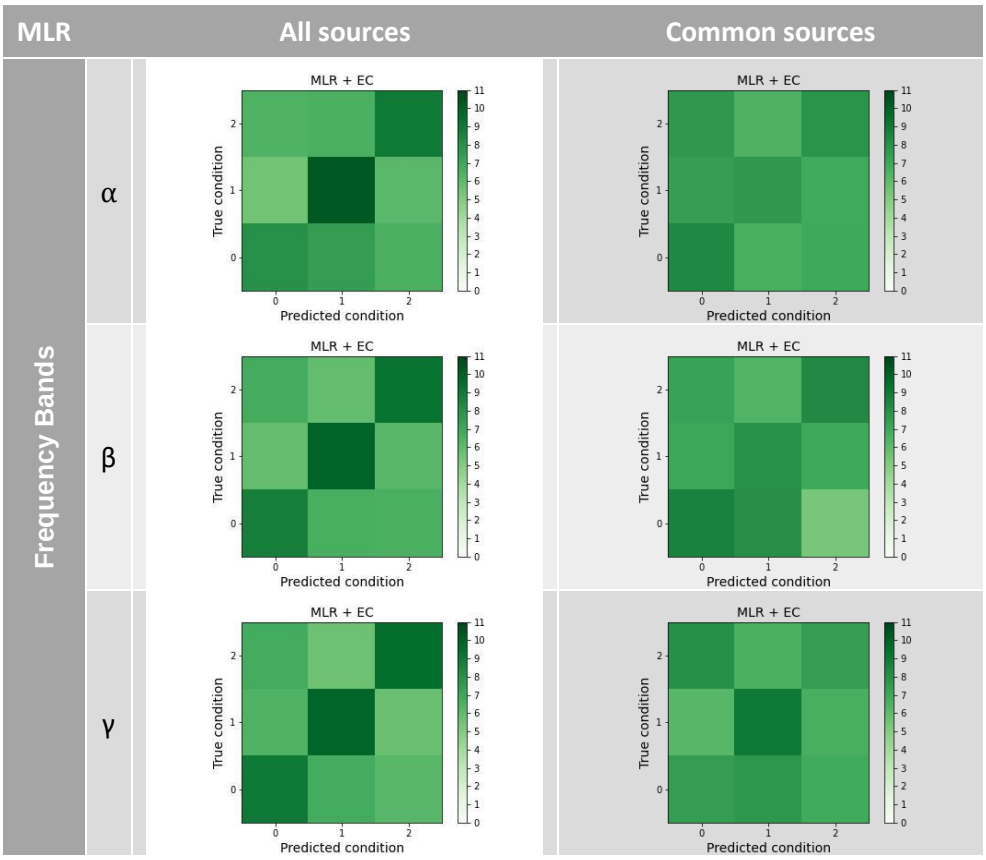
MLR
All sources
Common sources
Frequency Bands
α
β
γ
MLR + EC
True condition
Predicted condition

1NN		All sources	Common sources
Frequency Bands	α	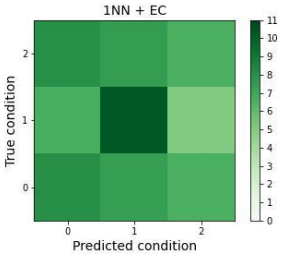	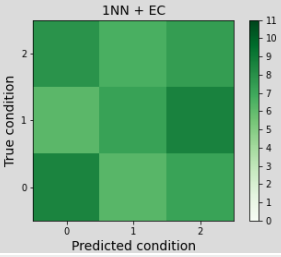
	β	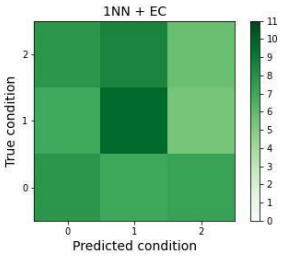	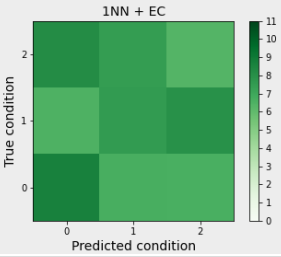
	γ